Mon. Not. R. Astron. Soc. **000**, 1–12 (2005) Printed 5 February 2008 (MN LATEX style file v2.2)

Properties of Intra-group Stars and Galaxies in Galaxy Groups: "Normal" versus "Fossil" Groups

Jesper Sommer-Larsen⋆
Dark Cosmology Centre, Niels Bohr Institute, University of Copenhagen, Juliane Maries Vej 30, DK-2100 Copenhagen, Denmark

Accepted —. Received —; in original form 2005 October 31

ABSTRACT

Cosmological (ΛCDM) TreeSPH simulations of the formation and evolution of twelve galaxy groups of virial mass $\sim 10^{14} M_{\odot}$ have been performed. The simulations invoke star formation, chemical evolution with non-instantaneous recycling, metallicity dependent radiative cooling, strong star-burst driven galactic super-winds and effects of a meta-galactic UV field. The intra-group (IG) stars are found to contribute 12-45% of the total group B-band luminosity at z=0. The lowest fractions are found for groups with only a small difference between the R-band magnitudes of the first and second ranked group galaxy ($\Delta m_{12,R} \lesssim 0.5$), the larger fractions are typical of "fossil" groups (FGs, $\Delta m_{12,R} \geq 2$). A similar conclusion is obtained from BVRIJK surface brightness profiles of the IG star populations. The IG stars in the 4 FGs are found to be older than the ones in the 8 "normal" groups (nonFGs), on average by about 0.3-0.5 Gyr. The typical colour of the IG stellar population is B-R=1.4-1.5, for both types of systems in good agreement with observations. The mean Iron abundance of the IG stars is slightly sub-solar in the central part of the groups ($r \sim 100$ kpc) decreasing to about 40% solar at about half the virial radius. The IG stars are α-element enhanced with a trend of [O/Fe] increasing with r and an overall [O/Fe]$\sim$0.45 dex, indicative of dominant enrichment from type II supernovae. The abundance properties are similar for both types of systems. The velocity distributions of the IG stars are, at $r \gtrsim 30$ kpc, significantly more radially anisotropic for FGs than for the nonFGs; this also holds for the velocity distributions of the group galaxies. This indicates that an important characteristic determining whether a group becomes fossil or not, apart from its formation time, as discussed by D'Onghia et al., is the "initial" velocity distribution of the group galaxies. For FGs one can dynamically infer the (dark matter dominated) mass distribution of the groups all the way to the virial radius, from the kinematics of the IG stars or group galaxies. For the nonFGs this method overestimates the group mass at $r \gtrsim 200$ kpc, by up to a factor of two at the virial radius. This is interpreted as FGs being, in general, more relaxed than nonFGs. Finally, FGs of the above virial mass should host $\sim$500 planetary nebulae at projected distances between 100 and 1000 kpc from the first ranked galaxy. All results obtained appear consistent with the tidal stripping and merging scenario for the formation of FGs, put forward by D'Onghia et al.

Key words: cosmology: theory — cosmology: numerical simulations — galaxies: groups — galaxies: formation — galaxies: evolution

1 INTRODUCTION

Hierarchical structure formation theories predict that the field star populations of haloes of galaxies like the Milky Way should consist partly of stars originally born in small proto-galaxies and later tidally stripped from these by the main galaxy or through interaction with other proto-galaxies. The halo stars resulting from tidal stripping or disruption of a proto-galaxy will stay localized in phase-space for a long period and several such "streams" of halo stars have been detected in the haloes of the Milky Way and M31 (e.g., Helmi et al. 1999; Ferguson et al. 2002).

From the point of view of structure formation, galaxy groups or clusters can be seen as scaled up versions of galaxies in hierarchical scenarios. In particular, tidal gravity fields will strip/disrupt galaxies in the group or cluster in a sim-

⋆ E-mail: jslarsen@tac.dk

ilar way as satellite galaxies in galaxy haloes, and a population of intra-group or -cluster (IG/IC) stars should thus at present reside between the group or cluster galaxies. It has been known for decades that cD galaxies are embedded in extended envelopes presumed to consist of stars tidally stripped off galaxies in the process of being engulfed by the cD (e.g., Oemler 1976; Dressler 1979). In recent years it has been possible to perform quantitative studies of these stellar envelopes through ultra-deep surface photometry of the general stellar population (e.g., Gonzalez et al. 2000; Gonzalez, Zabludoff & Zaritsky 2005; Feldmeier et al. 2002, 2004a; Mihos et al. 2005), or imaging/spectroscopy of individual planetary nebulae (PNe) (e.g., Arnaboldi et al. 2002, 2003; Feldmeier et al. 2004b) or supernovae Type Ia (Gal-Yam et al. 2003). The potential importance of intra-cluster stars in relation to the chemical enrichment of the intra-cluster medium (ICM) was recently discussed by Zaritsky, Gonzalez & Zabludoff (2004) and Lin & Mohr (2004).

Napolitano et al. (2003) have used an N-body dark matter only fully cosmological simulation of the formation of a Virgo-like cluster to make predictions about intra-cluster stars. They find that unrelaxed velocity distributions and (bulk) streaming motions of the IC stars should be common due to the large dynamical timescales in clusters. The dark matter only simulations have been complemented by various N-body simulations which invoke a more realistic modeling of the stellar properties of galaxies in order to study their fate in a cluster environment. In relation to the properties of the IC stars, recent progress has been made by Dubinski et al. (2003), and Feldmeier et al. (2004a).

In general the properties of the system of IC stars are set by two main effects: a) the cool-out of gas and subsequent conversion of cold, high-density gas to stars in individual galaxies and b) the stripping/disruption of the galaxies through interactions with other galaxies and the main cluster potential. Since such interactions will generally affect the star-formation rate (as long as a reservoir of gas is available) the former process is intimately coupled to the latter. Only fairly recently has it been possible to carry out fully cosmological gas-dynamical/N-body simulations of the formation and evolution of galaxy clusters at a sufficient level of numerical resolution and physical sophistication that the cool-out of gas, star-formation, chemical evolution and gas inflows and outflows related to individual cluster galaxies can be modeled to, at least some, degree of realism (e.g., Valdarnini 2003, Tornatore et al. 2004, Romeo et al. 2005a,b), though the problem of excessive, late time central cooling flows remains. Recently such simulations have been analyzed with emphasis on the properties of the IC stars (Murante et al. 2004, Willman et al. 2004, Sommer-Larsen, Romeo & Portinari 2005, SLRP05). Main observed properties of the IC light, such as the global IC light fractions of ∼20% (e.g., Arnaboldi 2004), and the patchy distribution of IC light can be reproduced, giving such simulations some credibility, also in relation to modeling the stripping and disruption of galaxies in the cluster environment.

Work on intra-group light/stars is much more in its infancy. Using PNe Castro-Rodriguez et al. (2003) and Feldmeier et al. (2004c) estimate IG light (IGL) fractions of just a few percent for the Leo and M81 groups, respectively. On the other hand, Da Rocha & Mendes de Oliveira (2005) find a large range, 0-46%, from broad band imaging of 3 compact groups, and for yet another Hickson Compact group White et al. (2003) found an IGL fraction of 38-48%. Gonzales and collaborators find that the combined luminosity of the brightest galaxy and the IG/IC light is about 40-60% of the total for both groups and clusters. The above authors all study "normal" groups, as opposed to the fairly recently discovered class dubbed "fossil" groups (FGs), first discovered using the ROSAT X-ray satellite by Ponman et al. (1994). FGs are characterized by a bright central galaxy (BG1), and a gap in the R-band luminosity function of at least two magnitudes, to the second brightest galaxy (BG2), and have been detected up to a redshift of at least 0.6 (Ulmer et al. 2005).

This paper represents the first detailed theoretical study of the IG light/stars, based on fully cosmological gas-dynamical/N-body simulations. The paper builds on the work of D'Onghia et al. (2005), who performed high-resolution simulations of a sample of twelve (fairly massive) groups of virial mass $\sim 10^{14}$ $M_\odot$ and virial (X-ray) temperature ~ 1.5 keV. The groups were selected essentially randomly, from a large cosmological simulation. D'Onghia et al. interpret the FG phenomenon in terms of the hierarchical structure formation scenario, such that FGs are groups which assemble their dark matter haloes earlier than "normal" groups. This leaves sufficient time to cause (second ranked) $L \sim L_*$ galaxies, initially orbiting in the groups, to reach the central parts due to dynamical friction, (mainly) against the dark matter. During this, the galaxies are tidally stripped, and finally disrupted and engulfed by the BG1[1]. One would hence expect, that the IG light/star fraction in FGs would be somewhat larger than in non-fossil groups (nonFGs).

Here, the properties of the IG light/stars and group galaxies are discussed on the basis of the simulations described above, with particular emphasis on comparing FGs to nonFGs. Results on IG star/group galaxy formation epochs, multi-band surface brightness profiles, colours, abundances, kinematics and dynamics are presented.

Section 2 briefly describes the code and the numerical simulations, in section 3 the results obtained are presented and discussed, and finally section 4 constitutes the conclusions.

2 THE CODE AND SIMULATIONS

Simulations of twelve galaxy group-sized dark matter haloes in the low-density, flat cold dark matter (ΛCDM scenario) with Ω_M=0.3, Ω_Λ=0.7, h =H_0/100 km s^{-1} Mpc^{-1}=0.7 and σ_8=0.9, were performed using the TreeSPH code briefly described in SLRP05. The code incorporates the "conservative" entropy equation solving scheme of Springel & Hernquist 2002; chemical evolution with non-instantaneous recycling of gas and heavy elements tracing 10 elements (H, He, C, N, O, Mg, Si, S, Ca and Fe; Lia, Portinari & Carraro 2002a,b); atomic radiative cooling depending on gas metal abundance and a redshift dependent, meta-galactic

[1] Computer animations of the formation of a "normal" group and a "fossil" group can be downloaded from http://www.tac.dk/~jslarsen/Groups

UV field; continuing, strong galactic winds driven by starbursts (SNII), optionally enhanced to mimic AGN feedback; and finally thermal conduction. A fraction f_W of the energy released by SNII explosions goes initially into the ISM as thermal energy, and gas cooling is locally halted to reproduce the adiabatic super–shell expansion phase; a fraction of the supplied energy is subsequently (by the hydro code) converted into kinetic energy of the resulting expanding superwinds and/or shells.

The original dark matter (DM)-only cosmological simulation, from which the groups have been drawn and resimulated at higher mass and force resolution, was run with the code FLY (Antonuccio-Delogu et al. 2003), for a cosmological box of $150h^{-1}$Mpc box-length. When re-simulating with the hydro-code, baryonic particles were "added" adopting a global baryon fraction of $f_b = 0.12$. The mass resolution was increased by up to 2048 times, and the force resolution by up to 13 times (see below). The initial redshift for the cosmological run, as well as for the group re-simulations, was z_i=39.

Twelve groups were randomly selected for resimulation. The only selection criterion was that the groups should have virial masses close to (within 10%) 1x10^{14} M$_\odot$, where the virial mass is the mass at z=0 inside the virial radius, defined as the region for which the average mass density is 337 times the average of the Universe (e.g., Bryan & Norman 1998). The corresponding virial radius is about 1.2 Mpc, and the virial (X-ray) temperature is about 1.5 keV. The purpose of this project was to study a cosmologically representative sample of groups, so no prior information about merging histories, was used in the selection of the 12 groups.

Particle numbers were about 250-300.000 SPH+DM particles at the beginning of the simulations increasing to 300-350.000 SPH+DM+star particles at the end. A novelty was that each star-forming SPH particles of the initial mass is gradually turned into a total of 8 star-particles. This considerably improves the resolution of the stellar component. SPH particles, which have been formed by recycling of star-particles, will have an eight of the original SPH particle mass — if such SPH particles are formed into stars, only one star-particle is created. As a result the simulations at the end contain star-particles of mass m_*=3.1x10^7 h^{-1}M$_\odot$, SPH particles of masses $m_{\rm gas}$=3.1x10^7 and 2.5x10^8 h^{-1}M$_\odot$, and dark matter particles of $m_{\rm DM}$=1.8x10^9 h^{-1}M$_\odot$. Gravitational (spline) softening lengths of 1.2, 1.2, 2.5 and 4.8 h^{-1}kpc, respectively, were adopted.

To test for numerical resolution effects one of the 12 groups (a "fossil" group) was in addition simulated at eight times (4 for star-particles) higher mass and two times (1.6 for star-particles) higher force resolution, than the "standard" simulations, yielding star-particle masses m_*=7.8x10^6 h^{-1}M$_\odot$, SPH particle masses $m_{\rm gas}$=7.8x10^6 and 3.1x10^7 h^{-1}M$_\odot$, dark matter particle masses $m_{\rm DM}$=2.3x10^8 h^{-1}M$_\odot$, and gravitational (spline) softening lengths of 0.76, 0.76, 1.2 and 2.4 h^{-1}kpc, respectively.. For this simulation particle numbers are about 1.400.000 SPH+DM particles at the beginning of the simulation increasing to 1.600.000 SPH+DM+star particles at the end.

In previous simulations of galaxy clusters (Romeo et al. 2005a,b, SLRP05) it was found that in order to get a sufficiently high ICM abundance a combination of a large value of f_W and a fairly top-heavy initial mass function (IMF) has to be employed. For the present simulations the "standard" parameters described in the above works: f_W=0.8, an IMF of the Arimoto-Yoshii type, and zero conductivity. The existence of narrow "cold fronts", observed in the many clusters, indicates that thermal conduction is generally strongly suppressed in the ICM. Moreover, it has previously been found that runs with a conductivity of 1/3 of the Spitzer value, and runs with zero conductivity yield very similar results for the stellar components (Romeo, et al. 2005a)

3 RESULTS AND DISCUSSION

This section presents results for the 12 groups, at z=0, mainly run at "standard" numerical resolution.

A well known problem in the modelling of galaxy groups and clusters, is the development of late-time cooling flows with bases at the position of BG1 and associated, central star-formation rates, which are too large compared to observations. In calculating the optical properties of the group galaxies a crude correction for this is made by removing all stars formed at the base of the cooling flow since redshifts $z_{\rm corr}$ = 2 or 1. Both redshifts correspond to times well after the bulk of the group stars have formed. The correction amounts to 20-40% in terms of numbers of BG1 stars. Using $z_{\rm corr}$ = 2 or 1 results in minor differences, so $z_{\rm corr}$=2 is adopted in this paper — for further discussion of this point see Sommer-Larsen et al. (2005). In cases where a similar correction of BG2 is appropriate (typically for non fossil groups, where BG2 enters into the main dark matter halo fairly late, $z \lesssim 0.5$), BG2 is corrected as well. These corrections are quite minor, $\lesssim$10% in terms of numbers of stars (D'Onghia et al. 2005).

At z=0, 1.7x10^4-2.9x10^4 star particles are located inside of $r_{\rm vir}$ $\simeq$1200 kpc (to within $\sim$3%) in the 12 groups simulated at standard resolution, and 9.3x10^4 star particles are located inside of $r_{\rm vir}$ of the FG simulated at high resolution. The corresponding masses in star particles are 5.3x10^{11}-9.0x10^{11} h^{-1}M$_\odot$ or a fraction of about 1% of the total virial mass In the following star particles will be referred to simply as "stars". The calculation of stellar luminosities is briefly described in section 3.2.

Eight of the groups are characterized by an R-band magnitude difference $\Delta m_{12,R}$ between the brightest (BG1) and second brightest (BG2) galaxy of less than 2 — following D'Onghia et al. (2005) these are classified as "normal" or "non fossil" groups (nonFGs). Four have a magnitude difference $\Delta m_{12,R} \geq 2$ — these are classified as "fossil" groups (FGs).

The effective radii of the BG1s, calculated from the B-band surface brightness profiles, are R_{eff} $\simeq$10-15 kpc, taking the inner 50 kpc of the groups as the extent of the BG1s — see below. The B-band absolute magnitudes of the BG1s lie in the range from -20.5 to -22.5. Compared to observations, $M_{\rm B}\sim$-21 corresponds to the brighter end of the luminosity function of ordinary groups (Khosroshahi et al. 2004), whereas $M_{\rm B}\sim$-22.5 corresponds to typical values for BG1s in fossil groups (Jones et al. 2003). Moreover,

from Kormendy (1977) it follows, that an elliptical galaxy of $M_{\rm B}\sim$-21.5 should have an R_{eff} $\sim$10 kpc, with a scatter of about a factor of two, in agreement with the above findings.

3.1 Identifying Group Galaxies and Intra-group Stars

Group galaxies were identified using the algorithm described in detail in SLRP05: a cubic grid of cube-length Δl=20 kpc was overlaid the group, and all cubes containing at least $N_{\rm th}$=10 stars are identified. Subsequently, each selected cube is embedded in a larger cube of cube-length $3\Delta l$. If this larger cube contains at least $N_{\rm min}$=15 star particles, which are gravitationally bound by its content of gas, stars and dark matter the system is identified as a potential galaxy. Since the method can return several, almost identical versions of the same galaxy only the one containing the largest number of star particles is kept and classified as a galaxy. The galaxy (stellar) mass resolution limit is about 5x10^8 $h^{-1}{\rm M}_\odot$ for the normal resolution runs, and 6x10^7 $h^{-1}{\rm M}_\odot$ for the high resolution run.

For the FGs an average of 12 galaxies (including the BG1) are found inside the virial radius to the resolution limit of M_B $\sim$ -18.5. For the nonFGs the corresponding number is 14. For the high-resolution run of a FG, 70 galaxies are identified to the resolution limit M_B $\sim$ -16.5.

There are no galaxies closer than $r_{\rm BG1}$=50 kpc to the BG1 in either of the twelve z=0 frames (this is not true in all z $\sim$0 frames, though, but it was tested that the results presented in the following did not depend on which z $\sim$ 0 frame was chosen to represent the present epoch).

The system of IG stars is defined as the stars located at BG1 distances $r_{\rm BG1} \leq r \leq r_{\rm vir}$ and *not* inside of the tidal radius of any galaxy in the group. The tidal radius for each galaxy is taken to be the Jacobi limit

$$r_J = \left(\frac{m}{3M}\right)^{1/3} D \quad , \qquad (1)$$

where m is the mass of stars, gas and dark matter in the galaxy (inside of r_J), D is the distance from the BG1 to the galaxy and M is the total mass of the group inside of D (e.g., Binney & Tremaine 1987). The BG1 itself is effectively just the inward continuation of the system of IG stars, so the division between IG and BG1 stars is somewhat arbitrary (hence below intra-cluster star fractions for $r_{\rm BG1}$=50 as well as 100 kpc are quoted). The above definition of IG stars is conservative, since the tidal radii are calculated on the basis of the z=0 frame BG1 distances of the galaxies. For any galaxy which has been through at least one peri-center passage, this tidal radius should be taken as a firm upper limit. Moreover, some IG stars will be inside of the tidal radius of one of the group galaxies just by chance. As the total "tidal volume" of all the group galaxies is found to be on average less than ten percent of the group virial volume, this effect can be neglected to a good first approximation.

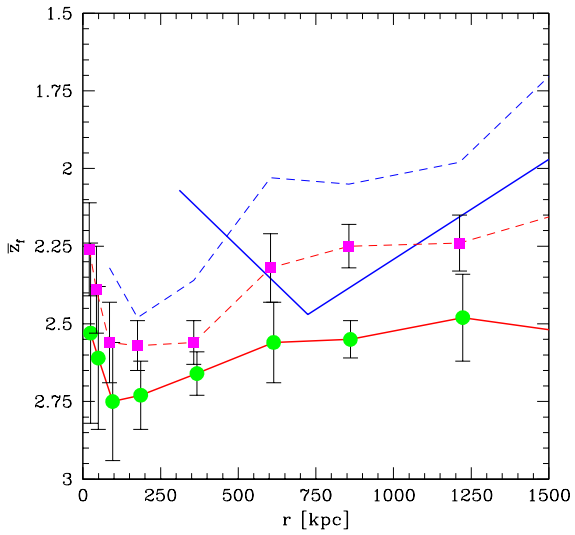

Figure 1. Mean redshift of formation of the BG1+IG stars (circles connected by solid line) and stars in galaxies (solid line) for the four FGs. Dashed lines and squares show the same for the eight nonFGs. The 1-σ uncertainties on $\bar{z}_f$ for the BG1+IG stars have been calculated on the basis of the system to system variation for the 4 FGs and 8 nonFGs, respectively (poisson errorbars, based on the numbers of stars in each bin, are much smaller). The uncertainties on $\bar{z}_f$ for the stars in nonFG galaxies are similar to the uncertainties for the FG/nonFG IG+BG1 stars; for the stars in FG galaxies they are somewhat larger.

3.2 The Intra-group Light Fraction

For comparison with observations it is relevant to determine stellar *luminosity* fractions, rather than mass fractions. Since ages and metallicities are available for all star particles, the photometric properties are straightforward to calculate treating each star particle as a Single Stellar Population (SSP; see Romeo et al. 2005a for details). SSP luminosities are computed by mass-weighted integration of the Padova isochrones (Girardi et al. 2002), according to the Arimoto-Yoshii IMF. For $r_{\rm BG1}$=50 kpc it is found that the IG stars contribute 20-45% of the group B-band luminosities, with the lower value typical for nonFGs with small $\Delta m_{12,R}$, and the larger for FGs (adopting instead $r_{\rm BG1}$=100 kpc, the IGL fractions decrease to 0.12-0.25). These IGL fractions are typical of what is found observationally for galaxy clusters (e.g., Arnaboldi 2004). Only a few observational studies of IGL in groups are presently available, and they all refer to "normal" groups (nonFGs). Estimates of the IGL fraction in such systems range from a few percent (Leo Group, Castro-Rodriguez et al. 2003; M81 Group, Feldmeier et al. 2004c), 0-46% (Hickson Compact Groups 79, 88 and 95; Da Rocha & Mendes de Oliveira 2005) to almost 50% (HCG 90, White et al. 2003). Gonzalez and collaborators find for their sample of 26 clusters and groups, spanning a range of velocity dispersions of 200-1100 km/s, that the combined BG1+IGL amounts to 40-60% of the total (Anthony Gonzales 2005, private communication). Evidently the system to system variation is very large,

which is in line with the findings in this paper (section 3.3). Moreover, one expects the projected distribution of IGL to be patchy (section 3.7), which adds to the observational scatter, as the fields surveyed usually do not cover the entire group.

3.3 Mean Formation Redshifts, Surface Brightness Profiles and Colours of the Intra-group Stars

Figure 1 shows the mean (spherically averaged) redshift of formation, $\bar{z}_f$, of the BG1 + IG stars and stars in galaxies (except the BG1) as a function of radial distance from the center of the BG1 for the FGs (solid lines) and nonFGs (dashed lines), respectively. The results presented here and in the following have been averaged over the 4 FGs and 8 nonFGs, respectively. For the FGs the average formation redshift of the IG stars is $\bar{z}_{f,IG} \sim 2.75$ at $r \sim$100-200 kpc, gradually decreasing to $\bar{z}_{f,IG} \sim 2.5$ at the virial radius. The IG stars in the nonFGs are on average somewhat younger (by about 0.2 in formation redshift). Qualitatively this is to be expected, since FGs are found to assemble earlier than nonFGs (D'Onghia et al. 2005), such that merging and stripping processes take place earlier; and also, such that the decrease in star-formation in the group galaxies in general, caused by ram-pressure stripping and other effects (see below) takes place earlier.

The stars in galaxies (except the BG1) are on average somewhat younger than the IG stars (by about 0.2-0.4 in formation redshift) for both types of groups. This seems reasonable, since the bulk of the IG stars originate in (proto) galaxies, which have been partly or fully disrupted through tidal stripping in the main group potentials or by galaxy-galaxy interactions. In contrast, the galaxies still remaining at z=0 have potentially been able to continue forming stars out of remaining cold gas or gas recycled by evolved stars and subsequently cooled to star-forming temperatures and densities. Still, due to ram-pressure stripping of the hot and dilute gas reservoir in galactic haloes and other effects, at least for cluster galaxies the star-formation rate decreases significantly from z=2 to 0, considerably more so than in field galaxies, cf. Romeo et al. (2005a).

Comparing to the results for intra-cluster stars in two cluster simulations discussed by SLRP05, it is found that the intra-cluster stars are somewhat older on average (with $\bar{z}_{f,IC} \sim$3) than the IG stars. Again this is to be expected, since clusters on average form from higher peaks in the initial cosmological fluctuations field, and hence experience "accelerated" galaxy formation relative to groups.

In Figure 2 is shown, for the 4 FGs and 8 nonFGs respectively, the median, azimuthally averaged BVRIJK surface brightness profiles of the BG1+IG stars (projection is along the z-axis, defined in section 3.5). The light profiles are approximately described by $r^{1/4}$ laws. The slope flattens slightly beyond $R \sim$100 kpc for both types of systems, at surface brightness levels of V$\sim$28 mag/arcsec^2, corresponding to about the limit which can be reached by surface photometry (e.g., Feldmeier et al. 2002). The median surface brightness of the FG BG1+IG stars at $R \sim$10-250 kpc is only

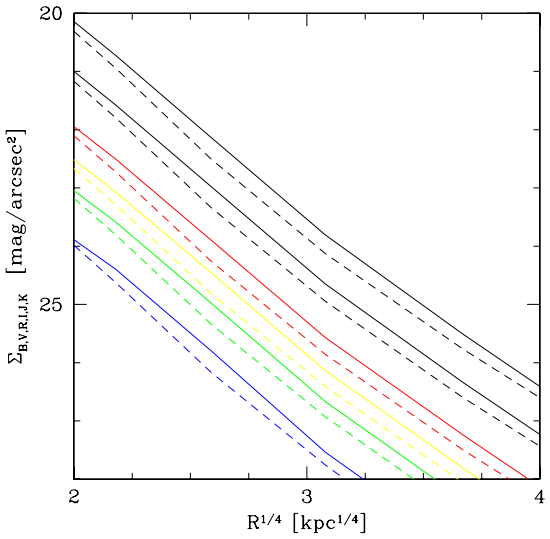

Figure 2. Azimuthally averaged multi-band (BVRIJK going bottom up) surface brightness profiles of BG1+IG stars for the FGs (solid lines) and nonFGs (dashed lines).

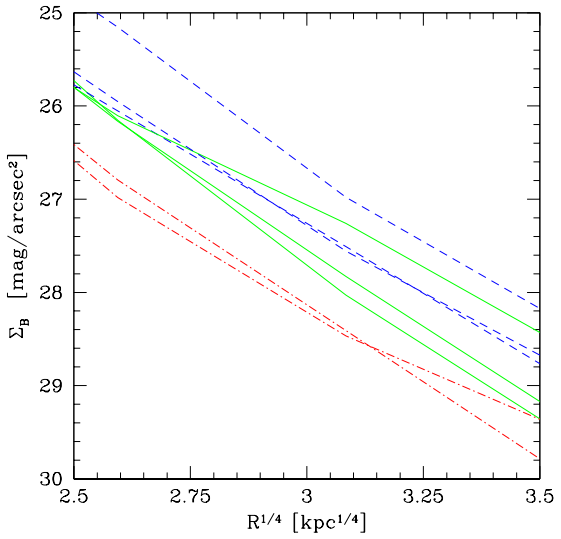

Figure 3. Azimuthally averaged B-band surface brightness profiles of the eight individual nonFGs, shown by dot-dashed lines for systems with $\Delta m_{12,R}$ <0.5 mag, solid lines for 0.5$\leq \Delta m_{12,R}$ <1 mag and dashed lines for 1$\leq \Delta m_{12,R}$ <2 mag The region shown on the x-axis corresponds to 39< R <150 kpc.

about 20-45% (0.2-0.4 mag) larger than that of the nonFG stars, but the variation in surface brightness between the individual nonFGs is quite large, about a factor of 5 ($\sim$1.7 mag) — see Figure 3. From the figure it is also seen that the groups with the smallest $\Delta m_{12,R}$ are characterized by the lowest surface brightness of IG stars, in agreement with the

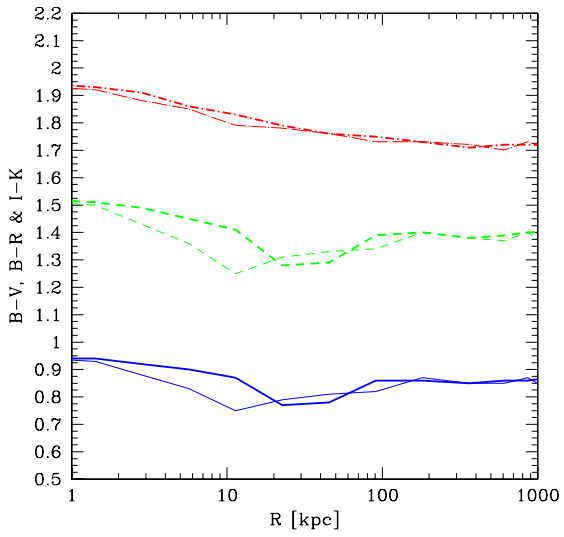

Figure 4. Azimuthally averaged B-V (solid lines), B-R (dashed lines) and I-K (dot-dashed lines) colours of the BG1+IG stars for the FGs (thick lines) and nonFGs (thinner lines), respectively.

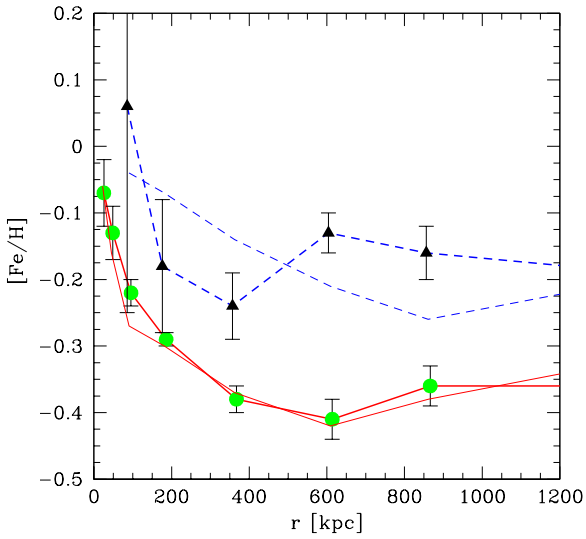

Figure 5. Spherically averaged iron abundance profile of BG1+IG stars (solid lines) and stars in group galaxies (dashed lines), shown for FGs by thick lines and nonFGs by thin lines, respectively (results for r <20 kpc are not shown for clarity).

notion that these are the least evolved systems, in terms of merging and relaxation.

Shown in Figure 4 are the azimuthally averaged B-V, B-R and I-K colours of the BG1+IG stars, for the FGs and nonFGs respectively. The profiles are almost flat (within 0.1 dex), in particular for B-V and B-R, and are very similar for the two types of systems. At ∼100 kpc $B-R \simeq 1.4$, typical of sub-L^* E and S0 galaxies (e.g., Gladders et al. 1998). Moreover, this is in the (albeit substantial) range of IGL colours found by Da Rocha & Mendes de Oliveira (2005) for 3 compact groups. There is at present no observational information available about colour gradients of IG stars in groups. It is interesting, however, that cluster cDs in general are found to have quite flat colour profiles, in some cases getting redder with R (e.g., Mackie 1992; Garilli et al. 1997; Gonzalez et al. 2000).

3.4 Abundance Properties of the Intra-group Stars and Group Galaxies

Figure 5 shows the spherically averaged profile of iron abundance of the BG1+IG stars, as well as of the stars in group galaxies, as a function of distance from the BG1. The results for the FGs and nonFGs are very similar: Iron is slightly subsolar in the BG1+IG stars at r ∼20 kpc and decreases to about 0.4 solar at large r; the stars in group galaxies follow a similar trend, but have about 0.2 dex higher iron abundance. Qualitatively this is reasonable, since the galaxies have had time to enrich their stellar population up to z=0, whereas the IG stars were formed in galaxies which were disrupted in the past. Durrell et al. (2002) carried out HST observations of an IC field in the Virgo cluster (which has a virial

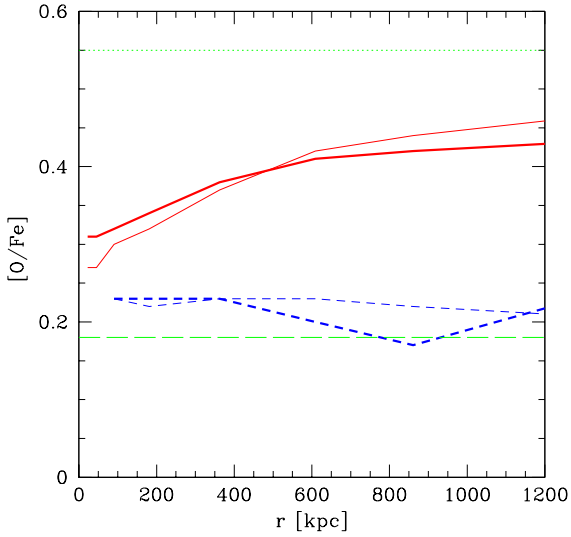

Figure 6. Spherically averaged oxygen-to-iron abundance ratio profile of BG1+IG stars (solid lines) and stars in group galaxies (dashed lines), shown for FGs by thick lines and nonFGs by thick lines, respectively. The limiting case for pure SNII enrichment, [O/Fe]=0.55, is shown by the thin, dotted line; the limit for complete SNII *and* SNIa enrichment, [O/Fe]=0.18, by thin, long-dashed line. (results for r <20 kpc are not shown for clarity).

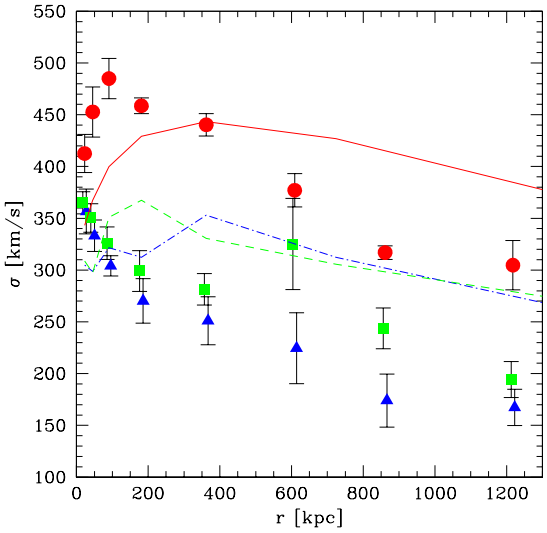

Figure 7. For BG1+IG stars in FGs (nonFGs) is shown the velocity dispersions σ_r by circles (solid line), σ_ϕ by squares (dashed line) and σ_θ by triangles (dot-dashed line). The statistical uncertainties, only shown for the FGs, are calculated based on system-to-system variations (cf. Fig.1). The uncertainties for the nonFGs are about a factor $\sqrt{2}$ smaller.

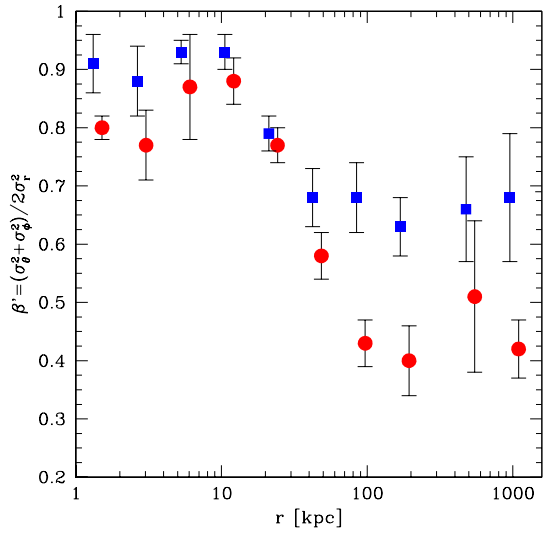

Figure 8. Velocity anisotropy parameter $\beta' = (\sigma_\phi^2 + \sigma_\theta^2)/2\sigma_r^2$ for BG1+IG stars for the FGs (circles) and nonFGs (squares). An isotropic velocity distribution has β'=1.

mass of only 2-3 times that of the groups considered here) at an average projected distance of 150 kpc from M87 (which for the purposes here can be assumed coincident with cluster center). They confirm an excess of red number counts, which they interpret as IC RGB stars. By comparison with observations of a dwarf irregular, they conclude that these stars have -0.8<[Fe/H]<-0.2, in quite good agreement with the results presented above.

Figure 6 shows the corresponding oxygen-to-iron ratios as a function of r. Again, the results for FGs and nonFGs are quite similar: [O/Fe] is super-solar everywhere for BG1+IG stars as well as galaxies, for the former being about 0.2 dex higher than for the latter. Both values lie in the range of present estimates for luminous elliptical galaxies in clusters. For IG/IC stars no observational information is currently available (Arnaboldi 2004, private communication).

For pure type II supernovae enrichment and with the Arimoto-Yoshii IMF, one expects $[O/Fe]_{SNII}$=0.55 (e.g., Lia, Portinari & Carraro 2002a), so it follows from Fig. 6 that SNe Ia do contribute somewhat to the enrichment of the BG1+IG stellar populations, and (not surprisingly) even more so for the stars still in galaxies at z=0 (in fact for an Arimoto-Yoshii IMF the global ($t \rightarrow \infty$) value of the SNII+SNIa enrichment is [O/Fe]=0.18).

The fact that iron abundances and oxygen-to-iron ratios are so similar in FGs and nonFGs for both IG stars and galaxies, indicates that the evolution in the two types of systems is quite similar, except that the formation of the FGs is accelerated relative to the nonFGs (cf. Fig. 1 and D'Onghia et al. 2005). In particular, the balance between the time-scale for SNII relative to SNIa production of iron and the time-scale for tidal stripping of IG stars must be similar in the two types of systems.

3.5 Kinematics of the Intra-group Stars and Group Galaxies

Using observed velocities of planetary nebulae it will ultimately be possible to kinematically "dissect" the systems of BG1+IG stars in nearby galaxy groups, like it is starting to be done for clusters, such as Virgo (e.g., Arnaboldi 2004; Feldmeier et al. 2004b). It is hence of considerable interest to determine for our simulations the kinematic properties of the BG1+IG stars, and of the group galaxies, for comparison. To this end the following approach is adopted: the individual groups are rotated in such a way that the minor axis of the BG1s at z=0 becomes the "z-axis" (but note that the galaxy groups as well as the BG1s are only slightly flattened at z=0). The four FGs and eight nonFGs are then centered at the BG1s and superposed for kinematic analysis. For each BG1+IG star and each group galaxy three perpendicular velocity components are determined: The radial component v_r=$\vec{v}\cdot\vec{e}_r$, where $\vec{e}_r$ is the unit vector pointing radially away from the center of the cluster, the perpendicular (tangential) component v_ϕ=$\vec{v}\cdot\vec{e}_\phi$, where $\vec{e}_\phi$ is the unit vector perpendicular to $\vec{e}_r$ and aligned with the x-y plane and the third (tangential) component v_θ=$\vec{v}\cdot\vec{e}_\theta$, where $\vec{e}_\theta$ is the unit vector $\vec{e}_\theta = \vec{e}_r \times \vec{e}_\phi$. The mean rotation $\bar{v}_\phi$ and velocity dispersions σ_r, σ_ϕ and σ_θ of BG1+IG stars and galaxies are calculated in spherical shells. As was found for the two simulated clusters analyzed by SLRP05, rotation is dynamically insignificant and will be ignored in the following analysis. Figure 7 shows the velocity dispersions of the BG1+IG stars as a function of radius for the FGs and nonFGs, respectively. As can be seen, the two tangential velocity dispersion are at all radii quite similar, confirming that the

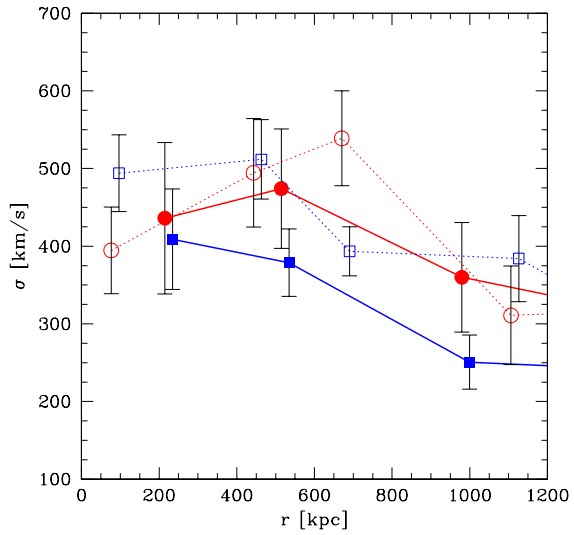

Figure 9. The radial and tangential velocity dispersions σ_r (circles) and $\sigma_t = \sqrt{(\sigma_\phi^2 + \sigma_\theta^2)/2}$ (squares) of the group galaxies are shown by filled and open symbols for the FGs and nonFGs, respectively. For clarity, the FG (nonFG) data are connected also by solid (dotted) lines. The statistical uncertainties are calculated for the two types of systems on the basis of the 45 and 105 galaxies in the FG and nonFG templates, respectively.

groups are only slightly flattened (alternatively the minor axis of the individual groups was oriented using the flattening of the entire groups, not just the BG1 — the groups were then again superposed, as above — this lead to results very similar to what is presented here). Secondly, except for the central region ($r \lesssim 30$ kpc) the velocity distributions are clearly radially anisotropic. This is quantified in Figure 8, which shows the radial dependence of the anisotropy parameter $\beta' = (\sigma_\phi^2 + \sigma_\theta^2)/2\sigma_r^2$, where β' is the ratio of the kinetic energy in mean tangential (1D) and radial motions, respectively (for an isotropic velocity distribution β'=1). In addition, it follows from the figure that the velocity distribution of the IG stars in the FGs is significantly more radially anisotropic than in the nonFGs. This is an important result in relation to understanding the fossil group phenomenon. D'Onghia et al. (2005) showed that the epoch of formation of a group is closely related to the "fossilness" of a group. The present result indicates that a second parameter may be the anisotropy of the "initial" velocity distribution of the group galaxies. The anisotropy of this distribution, as traced by the resulting IG stars at z=0, appears to relate to the "fossilness" of the group, in such a way that groups with highly radially anisotropic velocity distributions tend to become fossil. This seems quite reasonable in terms of a tidal stripping and merging scenario for the formation of fossil groups put forward by D'Onghia et al.

Figure 9 shows the velocity dispersions of the group galaxies as a function of radius for the FGs and nonFGs, respectively. Given the fairly small numbers of galaxies in the superposed systems, 45 in the FGs and 105 in the nonFGs (inside of the virial radius), only σ_r and $\sigma_t = \sqrt{(\sigma_\phi^2 + \sigma_\theta^2)/2}$ are shown. As was found by SLRP05, the velocity dispersions of the galaxies tend to be larger than for the IG stars. In particular, for the nonFGs σ_t for galaxies is considerably larger than for IG stars. Moreover, within the considerable statistical uncertainties, the velocity distribution of the galaxies in the nonFGs is more isotropic than for the FGs, as was found for the IG stars. This again hints that velocity distributions are of importance in relation to the formation of fossil groups.

Observationally, for the BG1+IG stars one will only be able to determine line-of-sight velocities using planetary nebulae, not full 3D velocities. For direct comparison with observations shown in Figure 10, for the FGs and nonFGs respectively, are the projected velocity dispersions of the BG1+IG stars, and (for comparison) of the dark matter, versus projected distance from the BG1. The results shown have been obtained by averaging over rings projected along the x, y and z directions.

For the FGs, the projected stellar velocity dispersion is ∼400 km/s at the group center, steadily decreasing to ∼200 km/s at the (projected) virial radius. For the nonFGs, which are less centrally concentrated, the projected stellar velocity dispersion is ∼300 km/s at the center, increases to ∼400 km/s at R ∼400 kpc and then decreases gradually with increasing R to about 275 km/s at projected $R_{\rm vir}$.

The projected velocity dispersions of the dark matter follows a similar trend with R as that of the stars, but are consistently larger. As the stars and dark matter are moving in the same gravitational potential this implies that the density distribution of dark matter is flatter than that of the BG1+IG stars (SLRP05).

3.6 Dynamical Determination of Group Mass Distributions using Intra-group Stars and Galaxies

It is of great interest to determine dynamical masses of groups and clusters, e.g., in relation to estimating the baryon fraction in such systems. The latter is of significant cosmological importance, as well as an important constraint which any successful model of group and cluster formation should meet. D'Onghia et al. (2005) showed that the dark matter haloes of FGs are assembled earlier than those of nonFGs. Given this, it seems reasonable to assume that FGs are dynamically more relaxed systems than nonFGs, and hence more suitable for dynamical mass estimation. To test this hypothesis the following approach is applied:
The equivalent of the hydrostatic equilibrium equation for a spherically symmetric, collision-less *stationary* (tracer) system in a spherical gravitational potential $\Phi(r)$ is the Jeans equation (e.g., Binney & Tremaine 1987)

$$\frac{d(n\sigma_r^2)}{dr} + \frac{2n}{r}\left(\sigma_r^2 - \sigma_t^2\right) = -n\frac{d\Phi}{dr} \quad , \qquad (2)$$

where $n(r)$ is the number density of the tracer system (in this case IG stars or galaxies). Eq.(2) can be recast in the form

$$\frac{d\ln(n\sigma_r^2)}{d\ln r} + 2\left(1 - \frac{\sigma_t^2}{\sigma_r^2}\right) = -\frac{r}{\sigma_r^2}\frac{d\Phi}{dr} = -\frac{GM_{\rm tot}(r)}{r\sigma_r^2} \quad , \qquad (3)$$

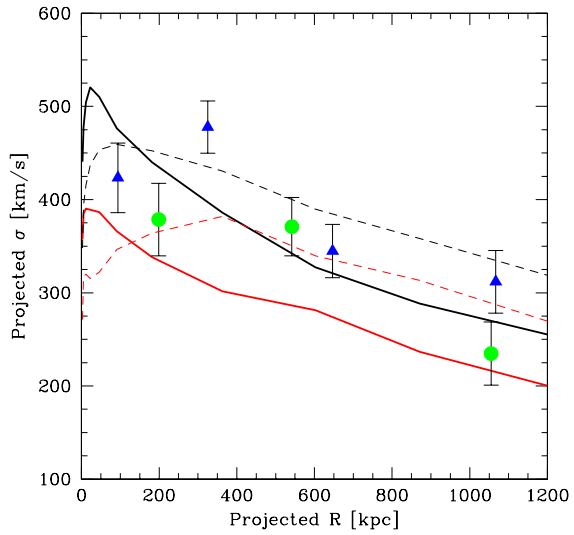

Figure 10. Projected velocity dispersions of the BG1+IG stars (lower curves) and, for comparison, the dark matter (upper curves), shown for the FGs by solid lines and for the nonFGs by dashed. Statistical uncertainties are $\Delta\sigma \lesssim 20$ km/s. Also shown are the projected velocity dispersions of the FG galaxies (circles) and nonFG galaxies (triangles).

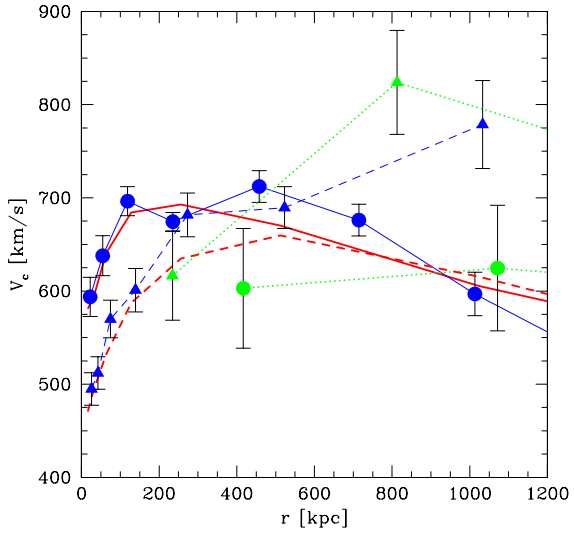

Figure 11. Equivalent circular speeds. Directly determined from the mass distributions of the FG and nonFG templates, using second part of eq.(4): FGs and nonFGs are shown by thick solid and dashed lines not connecting symbols, respectively. Dynamically inferred from the kinematic and spatial properties of the systems of IG stars, using last part of eq.(4): FGs and nonFGs are shown by solid and dashed lines connecting circles and triangles, respectively. Finally, shown by circles and triangles connected by dotted lines, are the same quantities, but inferred instead from the properties of the FG and nonFG galaxy populations.

where G is the gravitational constant and $M_{\rm tot}(r)$ is the cumulative total mass. In terms of the equivalent circular speed this can be expressed as

$$v_c^2 \equiv \frac{GM_{\rm tot}(r)}{r} = -\sigma_r^2 \left(\frac{d\ln(n\sigma_r^2)}{d\ln r} + 2\left(1 - \frac{\sigma_t^2}{\sigma_r^2}\right)\right) \qquad (4)$$

Assume that an observer of a galaxy group has full 3D information about the velocity field of the IG stars or galaxies. Then, in particular, $\sigma_r(r)$ and $\sigma_t(r)$ are known, rather than (from an observational viewpoint much more realistically) just the projected velocity dispersion. Moreover, assuming that $n(r)$ is known, then eq.(4) can be used to determine $v_c(r)$ or equivalently the total mass distribution. If the system under consideration is relaxed, and the potential as well as the system close to spherical, one should approximately recover the true, underlying mass distribution in this way.

The above approach is now applied to the FGs and nonFGs, respectively. The result of this exercise is shown in Figure 11: As can be seen, for the FGs both using IG stars and galaxies one recovers the true mass distribution, expressed through $v_c(r)$, quite well all the way to the virial radius, though the small number of galaxies in the FGs makes the mass determination using group galaxies somewhat uncertain. For the nonFGs, however, only in the inner (presumably most relaxed) parts of the groups, $r \lesssim 200$ kpc, one recovers the true mass distribution, whereas further out the above approach leads to an overestimate of the total mass. At the virial radius this overestimate approaches a factor of two. Note also, that due to the larger number of galaxies in the nonFG template, the mass estimate based on galaxies is somewhat more secure.

So it seems highly preferable to select FGs for purposes of observational baryon fraction estimation, mass estimation for comparison with gravitational lensing or X-ray estimated masses etc. This appears to be a very useful result, given that the measurement of the difference in luminosity of the first and second ranked galaxy in a group is straightforward.

3.7 Predicted Counts and Distributions of Intra-group Planetary Nebulae

In relation to upcoming searches for IG PNe it is of interest to predict what may result from such undertakings. The expected number of PNe expected per solar B-band luminosity of the stellar population is $\alpha_{1,B} = 9.4\ 10^{-9}$ PNe/$L_{B,\odot}$ (e.g., Arnaboldi et al. 2002; to be precise, this gives the number of PNe, within one B-band magnitude of the PNe luminosity function bright end cut). Based on this values Figure 12 shows the expected cumulative number of PNe within a ring of projected inner radius R and outer radius 1 Mpc for two systems: 1) the nonFG with the smallest projected B-band luminosity of the IG stars between 100 kpc and 1 Mpc, and 2) the FG with the largest corresponding luminosity. As can be seen the number count ratio is about a factor of three. Even for the first group a considerable number of PNe are expected to be found between 100 and 1000 kpc, about 200 PNe. However, two important points should be noted: Firstly, the projected distribution of PNe is expected to be patchy. This is illustrated in Figs. 13 and 14, which show the expected distributions of PNe projected along the z-axis for the two groups. In particular, for the nonFG, outside of about 100 kpc there are large coherent regions with

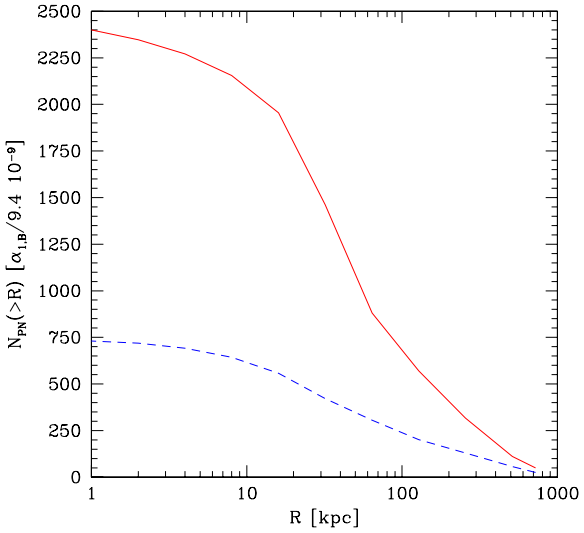

Figure 12. Cumulative number of PNe within a ring of projected inner radius R and outer radius 1 Mpc for two systems: 1) the nonFG with the smallest projected B-band luminosity of the IG stars between 100 kpc and 1 Mpc (dashed line) and 2) the FG with the largest corresponding luminosity (solid line).

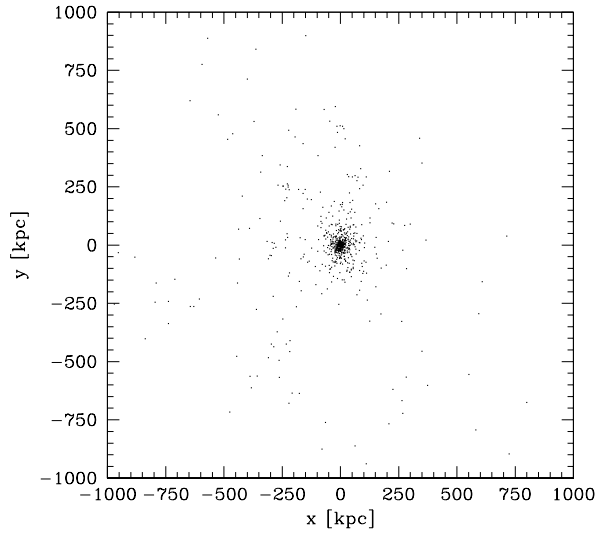

Figure 13. Projected distribution of PNe expected for the nonFG shown in Fig.12.

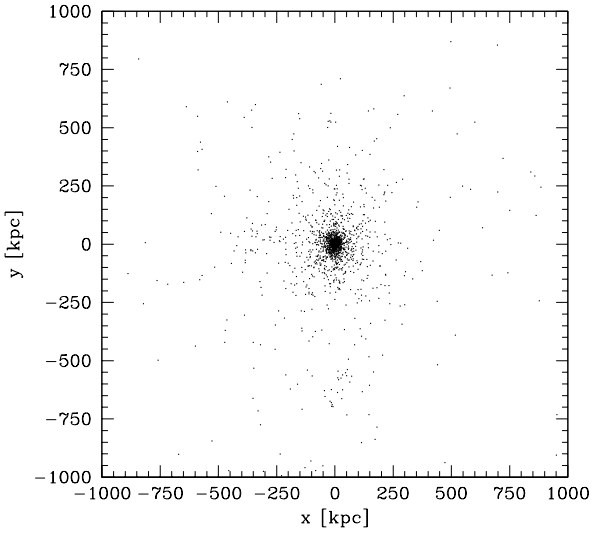

Figure 14. Projected distribution of PNe expected for the FG shown in Fig.12.

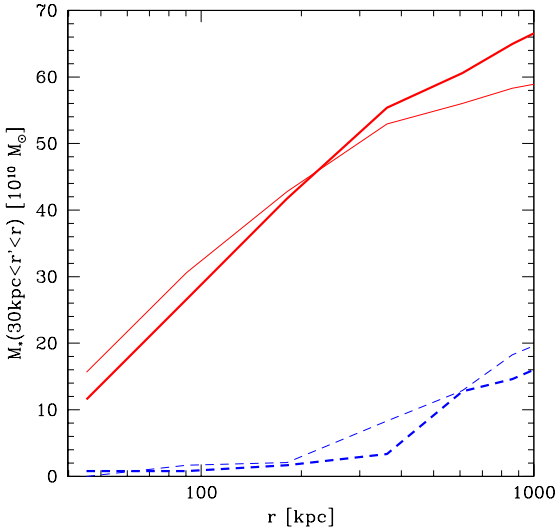

Figure 15. Cumulative mass of BG1+IG stars (solid lines) and in stars in group galaxies (dashed lines) outside of r=30 kpc for the normal resolution (thin lines) and high resolution (thick lines) simulations of a FG, respectively.

no PNe at all. Secondly, the values of $\alpha_{1,B}$ may vary by as much as a factor five (e.g., Castro-Rodriguez et al. 2003).

3.8 Numerical Resolution

It is important to test whether the properties of the IG star and galaxy populations presented in this paper depend on the numerical resolution of the simulations. To this end, as mentioned in section 2, one of the FGs was re-simulated at eight times higher mass and two times higher force resolution (4 and 1.6 times, respectively, for the star particles). This results in star-particle masses m_*=7.8x10^6 h^{-1}M$_\odot$, SPH particle masses $m_{\rm gas}$=7.8x10^6 and 3.1x10^7 h^{-1}M$_\odot$, dark matter particle masses $m_{\rm DM}$=2.3x10^8 h^{-1}M$_\odot$, and gravitational (spline) softening lengths of 0.76, 0.76, 1.2 and

2.4 h^{-1}kpc, respectively. Total particle numbers are about 1.400.000 SPH+DM particles at the beginning of the simulation increasing to 1.600.000 SPH+DM+star particles at the end.

In order to enable an optimal comparison between the normal and high resolution runs only Fourier modes up the Nyquist wavenumber of the normal resolution simulation were used to prepare the initial conditions for the high resolution run (i.e., additional high-wavenumber modes up to the Nyquist wavenumber of the high resolution simulation were *not* added to the Fourier modes).

Figure 15 shows the cumulative mass of BG1+IG stars and stars in galaxies outside of r=30 kpc for the normal and high resolution runs at z=0. There is good agreement between the runs — the somewhat larger mass in IG stars in the high resolution simulation at $r \gtrsim 200$ kpc is likely due to the better resolution of star-forming gas in the lower overdensity regions which come to populate the outer parts of the group. The flattening of $M(< r)$ with increasing r is due to the decrease in tidal stripping efficiency with r (SLRP05).

Very good agreement between other quantities, such as velocity dispersions, galaxy luminosity functions, chemical properties etc. is also found, as mentioned by D'Onghia et al. (2005). A detailed comparison will be presented in a forthcoming paper (D'Onghia et al., in preparation). Moreover, a high resolution simulation of one of the nonFGs is also in progress.

4 CONCLUSIONS

This work discusses the z=0 properties of the intra-group (IG) light/stars, as well as, mainly kinematic and dynamical, properties of the group galaxies. The results are based on fully cosmological, N-body/hydrodynamical simulations of 12 galaxy groups. Physical processes treated, include metal-dependent atomic radiative cooling, star-formation, supernova driven galactic super-winds, non-instantaneous chemical evolution and the effects of a meta-galactic, redshift dependent UV field. In relation to modeling the properties of the IG stars, as well as galaxy groups in general, this is an important step forward with respect to previous theoretical works.

The main results obtained, in particular in relation to comparing FGs to nonFGs, are as follows:

The intra-group (IG) stars are found to contribute 12-45% of the total group B-band luminosity at z=0. This is in agreement with some estimates of the IGL fraction, but too large compared to other studies, partly based on planetary nebulae (PNe). The latter apparent disagreement might, however, be due to patchiness effects in the IGL as well as PNe distribution, as well as the intrinsic scatter in the B-band luminosity to PN number ratio, cf. section 3.7.

The IG stars in the FGs form at a mean redshift $\bar{z}_f$ ∼2.5-2.75; in nonFGs the formation redshift is smaller by about 0.2. The stars in galaxies (excluding the BG1) form on average at redshifts 0.2-0.4 less than the IG stars, for both types of systems.

BVRIJK surface brightness profiles of the BG1+IG stars are fairly well described by $r^{1/4}$ laws, slightly flattening at R ∼100 kpc, which is about the limiting projected radius to which the IGL can be probed by ultra-deep surface photometry at present. The median surface brightness of the FG BG1+IG stars at R ∼10-250 kpc is only about 30-50% larger than that of the nonFG stars, but the variation in surface brightness between the individual nonFGs is quite large, about a factor of 5. The nonFG groups with the smallest magnitude difference between the first and second ranked galaxy are characterized by the lowest surface brightness of IG stars. This is in line with the suggestion by D'Onghia et al. (2005), that these are the least evolved systems, in terms of merging and relaxation. The typical colour of the IG stellar population is, independent of system type, B-R=1.4-1.5, comparable to the colour of sub-L^* E and S0 galaxies, and in good agreement with estimates of the global colour of the IGL in compact groups.

For both types of systems, the mean Iron abundance of the IG stars is slightly sub-solar in the central parts of the groups ($r \lesssim 100$ kpc) gently decreasing to 40% solar at about half the virial radius. This is in line with the rather broad limits by Durrell et al. (2002) on the iron abundance of the IC stars in Virgo (which has a virial mass only 2-3 times larger than that of the simulated groups). The group galaxies are found to be on average about 0.2 dex more iron rich than the IG stars. The latter are α-element enhanced with, e.g, [O/Fe] increasing slightly with r and characterized by a typical [O/Fe]∼0.4 dex. The group galaxies have [O/Fe] closer to solar.

The velocity distribution of the IG stars is outside of the central region ($r \lesssim 30$ kpc) radially anisotropic, and, moreover, considerably more so for the FGs than in the nonFGs. This may indicate, that an important parameter in determining whether a group becomes fossil or not, apart from its dark matter halo assembly time (cf. D'Onghia et al. 2005), is the "initial" velocity distribution of its galaxies: the more radially anisotropic it is, the more "fossil" does the group become at z=0. This appears in line with the tidal stripping and merging scenario for the formation of fossil groups, put forward by D'Onghia et al. For the IG stars, the tangential velocity dispersion in the two perpendicular directions are similar at all radii, kinematically indicating that the groups are quite round. For the group galaxies the velocity dispersions are somewhat larger than for the IG stars, and, as for the IG stars, the velocity distribution of the FG galaxies is more radially anisotropic than for the nonFGs.

In relation to dynamical estimates of virial masses and mass distributions of galaxy groups using some tracer population, such as IG stars or galaxies, it is shown that provided one has information about both radial and tangential velocity dispersions, as well as the density profile of the tracer population, then for FGs one can recover quite well the underlying (mainly dark matter) mass distribution all the way to the virial radius, by applying Jeans' equation. On the contrary, for nonFGs, this only works in the inner parts of the groups, $r \lesssim 200$ kpc, further out it leads to an overestimate of the group mass, approaching a factor of about two at the virial radius. This is simply because Jeans' equation applies to *stationary* systems, which nonFGs are not, cf. D'Onghia et al. (2005).

Using the "standard" B-band luminosity to PN number conversion it is predicted that 200-700 PNe should be located between projected distances of 100 and 1000 kpc for $M_{\rm vir} \sim 10^{14} M_\odot$ groups. The lower number applies to nonFGs with small R-band magnitude gaps between the first

and second ranked galaxy, the higher to typical FGs. However, in particular for the former systems, the PN distribution is predicted to be highly patchy.

One FG was re-simulated at eight times higher mass and two times higher force resolution. Comparison with the standard resolution run of this FG indicates that the results presented in this paper are largely robust to resolution changes.

In summary, all results obtained appear consistent with the tidal stripping and merging scenario for the formation of FGs, put forward by D'Onghia et al. In general, one should find more IG light and PNe in FGs, so observational projects to this end deserve to be promoted, also for testing the predictions made in this paper. In particular, for dynamical determination of group masses, for comparison with estimates based on gravitational lensing or X-ray emission, or for baryon fraction estimation, FGs seem considerably more useful than nonFGs.

ACKNOWLEDGMENTS

I have benefited from comments by Elena D'Onghia, John Feldmeier, Ken Freeman, Anthony Gonzalez, Troels Haugbølle, Claudia Mendes de Oliveira, Kristian Pedersen, Trevor Ponman, Laura Portinari, Jesper Rasmussen, Alessio Romeo and the anonymous referee.

All computations reported in this paper were performed on the IBM SP4 and SGI Itanium II facilities provided by Danish Center for Scientific Computing (DCSC). This work was supported by the Villum Kann Rasmussen Foundation. The Dark Cosmology Centre is funded by the DNRF.

REFERENCES

Antonuccio-Delogu V., Becciani U., Ferro D., 2003, Comput. Phys. Commun., 155, 159
Arnaboldi, M., 2004, IAU Symp., **217**, Recycling intergalactic and interstellar matter, eds. P.-A. Duc, J. Braine, and E. Brinks., p.54
Arnaboldi, M. et al., 2002, AJ, 123, 760
Arnaboldi, M. et al., 2003, AJ, 125, 514
Binggeli, B., Tammann, G.A., & Sandage, A., 1987, AJ, 94, 251
Binney, J., & Tremaine, S. 1987, Galactic Dynamics. Princeton Univ. Press, Princeton
Borgani, S., 2004, MNRAS, 348, 1078
Bryan G.L., Norman M.L., 1998, ApJ 495, 80
Castro-Rodrguez, N., Aguerri, J. A. L., Arnaboldi, M., Gerhard, O., Freeman, K. C., Napolitano, N. R., & Capaccioli, M., 2003, A&A, 405, 803
Da Rocha, C., & Mendes de Oliveira, C., 2005, MNRAS, 364, 1069
D'Onghia, E., Sommer-Larsen, J., Romeo, A.D., Burkert, A., Pedersen, K., Portinari, L., & Rasmussen, J., 2005, ApJ, 630, L109
Dressler, A., 1979, ApJ, 231, 659
Dubinski, J., Koranyi, D., & Geller, M., 2003, IAU symposium, 208, 237
Durrell, P.R., Ciardullo, R., Feldmeier, J.J., Jacoby, G.H., & Sigurdsson, S., 2002, ApJ, 570, 119
Feldmeier, J.J., et al., 2002, ApJ, 575, 779
Feldmeier, J.J., et al., 2004a, ApJ, 609, 617
Feldmeier, J.J., Ciardullo, R., Jacoby, G.H., & Durell, P.R., 2004b, ApJ, 615, 196
Feldmeier, J.J., Ciardullo, R., Jacoby, G.H., Durell, P.R., & Mihos, J. C., 2004c, IAU Symposium 217, p.64
Ferguson, A.M.N., Irwin, M.J., Ibata, R.A., Lewis, G.F., & Tanvir, N.R., 2002, AJ, 124, 1452
Freeman, K.C., et al., 2000, ASP Conf. Series, 197, 389
Gal-Yam, A., et al., 2003, AJ, 125, 1087
Garilli, B., et al., 1997, AJ 113, 1973
Girardi, L., et al., 2002, A&A, 391, 191
Gladders, M.D., et al., 1998, ApJ, 501, 571
Gonzalez, A.H, et al., 2000, ApJ, 536, 561
Gonzalez, A.H, Zabludoff, A.I., & Zaritsky, D. 2005, ApJ, 618, 195
Helmi, A., White, S.D.M., de Zeeuw, P.T., & Zhao, H., 1999, Nature, 402, 53 Burke, D.J., 2003, MNRAS, 343, 627
Jones, L.R., et al. 2003, MNRAS, 343, 627
Khosroshahi, H.G. et al. 2004, MNRAS, 349, 527
Kormendy, J., 1977, ApJ, 218, 333
Lia, C., Portinari, L., & Carraro, G. 2002a, MNRAS, 330, 821
Lia, C., Portinari, L., & Carraro, G. 2002b, MNRAS, 335, 864
Lin Y.-T., Mohr J.J., 2004, ApJ, 617, 879
Mackie, G. 1992, ApJ 400, 65
McNamara, B. R. 2004, in "The Riddle of Cooling Flows in Galaxies and Clusters of Galaxies", Charlottesville, Virginia, USA, Eds. T.H.Ruprecht, J.C.Kempner & N.Soker
Mihos, C., Harding, P., Feldmeier, J.J., & Morrison, H., 2005, ApJL, in press, (astro-ph/0508217)
Murante, G., et al., 2004, ApJ, 607, L83
Napolitano, N.R., et al., 2003, ApJ, 594, 172
Oemler, A. Jr., 1976, ApJ, 209, 693
Ponman, T.J. et al. 1994, Nature, 369, 462
Romeo, A.D., Portinari, L., & Sommer-Larsen, J., 2005a, MNRAS, 361, 983
Romeo, A.D., Sommer-Larsen, J., Portinari, L., & Antonuccio, V., 2005b, MNRAS, submitted (astro-ph/0509504)
Sommer-Larsen, J., Beers, T.C., Flynn, C., Wilhelm, R., & Christensen, P. R. 1997, ApJ, 481, 775
Sommer-Larsen J., Götz M., Portinari L., 2003, ApJ, 596, 46
Sommer-Larsen, J., Romeo, A.D., & Portinari, L., 2005, MNRAS, 357, 478 (SLRP05)
Springel, V., & Hernquist, L., 2002, MNRAS, 333, 649
Tornatore, L., Borgani, S., Matteucci, F., Recchi, S., & Tozzi, P., 2004, MNRAS, 349, L19
Ulmer, M. P., et al., 2005, ApJ, 624, 124
Valdarnini, R., 2003, MNRAS, 339, 1117
White, P.M., Bothun, G., Guerrero, M.A., West, M.J., & Barkhouse, W.A., 2003, ApJ, 585, 739
Willman, B., Governato, F., Wadsley, J., & Quinn, T., 2004, MNRAS, 355, 159
Zaritsky, D., Gonzalez, A.H, & Zabludoff, A.I., 2004, ApJ, 613, L93